Metal-Oxygen Hybridization and Core-Level Spectra in Actinide and Rare-Earth Oxides

Jindřich Kolorenč

Institute of Physics, The Czech Academy of Sciences, Na Slovance 2, 182 21 Praha, Czech Republic

We employ a combination of the density-functional theory and the dynamical mean-field theory to study the electronic structure of selected rare-earth sesquioxides and dioxides. We concentrate on the core-level photoemission spectra, in particular, we illustrate how these spectra reflect the integer or fractional filling of the 4f orbitals. We compare the results to our earlier calculations of actinide dioxides and analyze why the core-level spectra of actinide compounds display a substantially reduced sensitivity to the filling of the 5f orbitals.

1. Introduction

Recently, we have used a combination of the density-functional theory and the dynamical mean-field theory, the so-called LDA+DMFT method, to investigate the electronic structure of three actinide dioxides, UO_2, NpO_2, and PuO_2 [1]. The theory indicates a large covalent mixing of the actinide 5f states with the 2p states of oxygen, which results in a substantially increased filling of the 5f orbitals away from the nominal integer occupation. The core-level spectroscopy is able to detect an analogous non-integer number of 4f electrons n_{4f} in many rare-earth compounds, including dioxides CeO_2 and PrO_2, and to distinguish this fractional filling from an integer filling that is characteristic, for instance, to rare-earth sesquioxides [2, 3]. The core-level spectra of the actinide dioxides, on the other hand, appear to be compatible with an integer number of 5f electrons [4]. For example, the 4f x-ray photoemission spectra (XPS) show only small shake-up satellites, whereas the 3d XPS in CeO_2, in which there is approximately one half of an electron in the 4f shell, has a very different three-peak shape. We argue that this difference does not point to an integer number of 5f electrons in the actinide dioxides but to a reduced sensitivity of the core-level spectra to the filling of the 5f orbitals. Our large deviations from the nominal integer filling are in fact compatible with the small shake-up satellites in 4f XPS when a detailed calculation is performed [1]. To put our theoretical findings on an even firmer ground, we apply the LDA+DMFT method to the electronic structure of selected rare-earth oxides with known fractional and near-integer n_{4f}, and analyze possible reasons for the reduced sensitivity of the core spectra to the 5f electron count in the actinide oxides.

2. Computational method

We employ the implementation of the LDA+DMFT method described in [1]. First, the non-magnetic LDA band structure, obtained with the aid of the *WIEN2k* code [5], is represented by a tight-binding hamiltonian in the basis of Wannier functions with lanthanide 6s, 4f, 5d, and oxygen 2p character [6, 7] Then, a spherically symmetric Coulomb vertex, parametrized by four Slater integrals (F_0, F_2, F_4, and F_6), is added to each of the 4f shells, and the resulting Hubbard model is solved using the dynamical-mean-field theory. In this theory, the many-body effects are taken into account only locally, separately for each of the 4f shells, by means of a momentum-independent self-energy. Evaluation of this self-energy amounts to a construction of an auxiliary impurity model that, in our implementation, is subsequently solved by the Lanczos method in a reduced Fock basis [1].

All calculations are performed for the experimental crystal structures. The sequioxides (Ce_2O_3, Pr_2O_3, and Nd_2O_3) crystallize in the hexagonal $P\bar{3}m1$ structure with oxygen atoms in 1a and 2d positions, $(0,0,0)$, $(1/3, 2/3, z)$, and $(2/3, 1/3, -z)$, and with lanthanide atoms in 2d positions, $(1/3, 2/3, z')$ and $(2/3, 1/3, -z')$. The cerium dioxide crystallizes in the cubic $Fm\bar{3}m$ structure with oxygen atoms in 8c positions, $(1/4, 1/4, \pm 1/4)$, and with cerium atom in 4a position, $(0, 0, 0)$. The numerical values of the lattice parameters are listed in Table 1.

The LDA electronic structure found with the *WIEN2k* code incorporates scalar-relativistic effects as well as the spin-orbit coupling. The calculations are performed with the following parameters: the radii of the muffin-tin spheres are $R_{MT}(Ce) = R_{MT}(Pr) = R_{MT}(Nd) = 2.42\,a_B$ for lanthanide atoms and $R_{MT}(O) = 1.9\,a_B$ for oxygen atoms, and the basis set cutoff K_{max} is defined with $R_{MT}(O) \times K_{max} = 7.5$. The Brillouin zone is sampled with 3610 k points in the sequioxides and with 3375 k points in the dioxide. The Slater parameters that define the Coulomb interaction in the Hubbard model are $F_2 = 11.9$ eV, $F_4 = 8.0$ eV, and $F_6 = 5.9$ eV. These parameters correspond to the Hund's exchange being $J = 1.0$ eV. The Coulomb $U = F_0$ is estimated as $U = 8.0$ eV in the sesquioxides, at the upper limit of the interval determined by constrained LSDA calculations [15]. The experimental spectra indicate that U in CeO_2 is slightly larger than in Ce_2O_3 [2] and we use

Table 1: Experimental lattice parameters of Ce_2O_3 [8], Pr_2O_3 [9], Nd_2O_3 [10], and CeO_2 [11], the DMFT filling of the 4f shell, and the DMFT gap compared to the gap measured in the optical absorption experiments (from [12, 13] for sesquioxides, and from [14] for CeO_2).

	a (Å)	b (Å)	z	z'	n_{4f}	DMFT gap (eV)	exp. gap (eV)
Ce_2O_3	3.888	6.063	0.648	0.251	1.09	2.5	2.4
Pr_2O_3	3.857	6.016	0.630	0.235	2.08	3.3	3.9
Nd_2O_3	3.827	5.991	0.646	0.247	3.07	3.9	4.7
CeO_2	5.410	—	—	—	0.40	3.0	3.2

$U = 10.0$ eV there. For the double-counting correction, which approximately subtracts the f–f Coulomb interaction included in the LDA band structure, we adopt the isotropic formula $U_{DC} = U\left(n_{4f} - 1/2\right) - J\left(n_{4f} - 1\right)/2$ from the so-called fully localized limit, where n_{4f} is the self-consistently determined number of 4f electrons.

The auxiliary impurity model that enters the DMFT calculations is approximated by its finite variant. Vaguely speaking, it corresponds to a cluster that includes the 4f shell and its nearest-neighbor ligand orbitals. Despite being relatively small, this finite model accurately represents the 4f shell and its environment in the insulating oxides [1]. Quantitatively, the coupling of the 4f shell to the surrounding electronic states (often referred to as the bath) is described by the so-called hybridization function Δ [16]. In our case, it is a 14×14 matrix spanning orbital and spin degrees of freedom of the f shell. Its trace in CeO_2 and Ce_2O_3 is shown in Figure 1. In the dioxide, the hybridization is dominated by the oxygen 2p states located below the Fermi level. Apparently, the Ce 5d and Ce 6s states could have been neglected as they were in the case of actinide dioxides in [1]. In the sesquioxide, the hybridization with the Ce 5d states is noticeably stronger and it is not a priori obvious if it does or does not play an important role. Therefore, we include bath orbitals describing the coupling to the oxygen 2p states (14 orbitals below the Fermi level) as well as bath orbitals modeling the coupling to the (next-nearest-neighbor) Ce 5d states (14 orbitals above the Fermi level) in our finite impurity model. The parameters of these bath orbitals, that is, their energy and coupling to the 4f shell, are determined by a procedure similar to [1].

3. Results and discussion

We focus mainly on the core-level spectra and hence we comment on the valence-band electronic structure only briefly. The filling of the 4f shell is listed in Table 1; as expected, it ends up near the nominal integer value in the sesquioxides, and close to one half in CeO_2. In this respect, CeO_2 and the actinide dioxides studied earlier are very similar [1]. Table 1 also shows the computed band gaps in comparison to their experimental values. The theory is very accurate in both cerium oxides, but it underestimates the gaps in Pr_2O_3 and Nd_2O_3. The problem is in the oxygen 2p and lanthanide 5d bands being too close to each other in the LDA electronic structure. Consequently, the calculated gap has the p–d character in Pr_2O_3 and Nd_2O_3, and the 4f states are below the valence-band maximum and above the conduction-band minimum. The LDA+DMFT method corrects for the correlation effects only in the 4f shell and leaves the other bands mostly untouched. This issue can be addressed by replacing LDA with a hybrid functional [17] or with the GW approximation [18].

In the rest of the paper we discuss the x-ray photoemission from core levels. The spectra are calculated in the
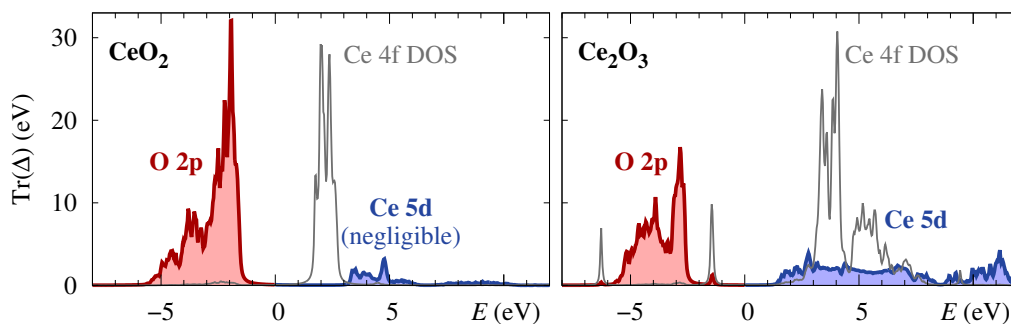

Figure 1: Trace of the hybridization function in CeO_2 (left) and Ce_2O_3 (right). The 4f density of states is shown as well. The curves correspond to the final LDA+DMFT solution. The hybridization below the Fermi level is due to the 2p states at the nearest-neighbor oxygen atoms, the hybridization above the Fermi level is mainly due to the cerium 5d bands.
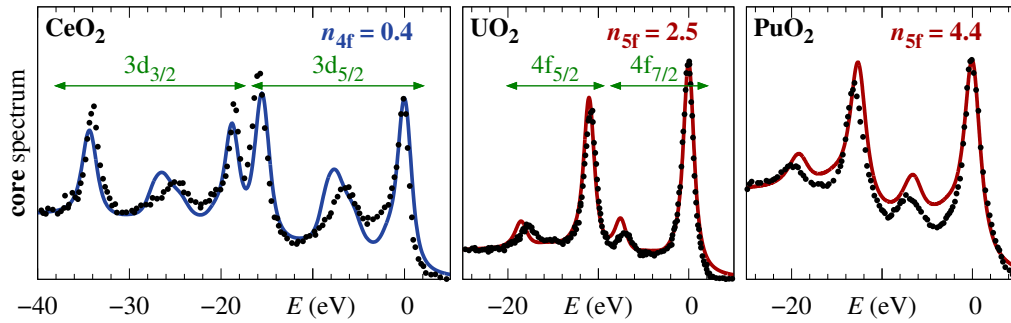
Figure 2: X-ray photoemission from the 3d core level in CeO_2 (this work) and from the 4f core level in UO_2 and PuO_2 (adopted from [1]). Lines come from the LDA+DMFT method, dots are experiments (CeO_2 from [22], UO_2 from [23], and PuO_2 from [24]). The life-time broadening of the theoretical spectra was adjusted in each compound separately so that the width of the line centered at zero energy matches the experiment. A background due to the secondarily scattered electrons was added to the theoretical curves as described in [21].

LDA+DMFT method following the observation that the auxiliary impurity model can be identified [19] with the impurity model of the charge-transfer ligand-field theory [20]. The details of our implementation are given in [1]; the spectra depend on a semi-empirical parameter U_{cv} that characterizes the strength of the Coulomb interaction between the core hole and the valence f electrons in the final state of the photoemission process. The core-valence Coulomb parameter is usually larger than the valence-band U [2, 20]. We set it as $U_{cv} = 1.2U$, that is, $U_{cv} = 12.0$ eV in CeO_2 and $U_{cv} = 9.5$ eV in the rare-earth sesquioxides.

Figure 2 shows the calculated and experimental XPS for three dioxides (CeO_2, UO_2, and PuO_2), all with approximately half-integer filling of the valence f shell. Figure 3 shows analogous spectra for three sesquioxides with nearly integer filling of the valence f shell. The theory does a good job in all cases, only the satellite located 5 eV from the main peak in Nd_2O_3 is too intense. We suspect that this discrepancy is related to the underestimated band gap (Table 1) that may lead to an overestimation of the hybridization effects. The fact that XPS can be very accurately modeled by the charge-transfer ligand-field theory is nothing new [2, 20, 21], the benefits of the LDA+DMFT are (a) in re-

duction of the number of empirical parameters since the hybridization is determined from first principles, and (b) in the core-level spectra being calculated on the same footing as the valence-band electronic structure.

Comparing the spectra plotted in Figure 2 and Figure 3, we see that there is an obvious difference between CeO_2 and the lanthanide sesquioxides. We could conclude that a core line split into two peaks is characteristic for an integer number of valence f electrons, and a core line split into three peaks is a sign of a fractional number of the f electrons. But where did the three peaks go in the actinide dioxides that also have a nearly half-integer number of 5f electrons, at least according to the theory [1, 25]? We believe that the answer is in Figure 4 where we investigate the dependence of the spectra on the magnitude of the core-valence Coulomb interaction U_{cv}. In the lanthanide oxides, this interaction is stronger and it thus causes a larger perturbation of the valence electronic structure in the final state of the photoemission process. The larger perturbation is necessary for unmasking the different fillings of the valence f shell. When the CeO_2 and Ce_2O_3 spectra are computed with a smaller $U_{cv} = 6.0$ eV, the value that was used in the actinide dioxides [1], the core lines display only a small shake-up
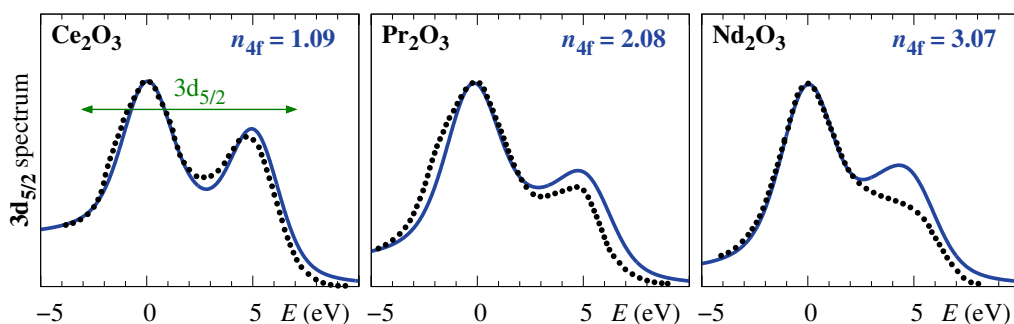

Figure 3: X-ray photoemission from the $3d_{5/2}$ core level in Ce_2O_3, Pr_2O_3, and Nd_2O_3 (lines). Details of the life-time broadening and background are the same as in Figure 2. The experimental data (dots) are adopted from [26].

Table 2: The valence histogram (weights w_n of the configurations with a given number of f electrons n) of three of the investigated oxides as determined by the LDA+DMFT method.

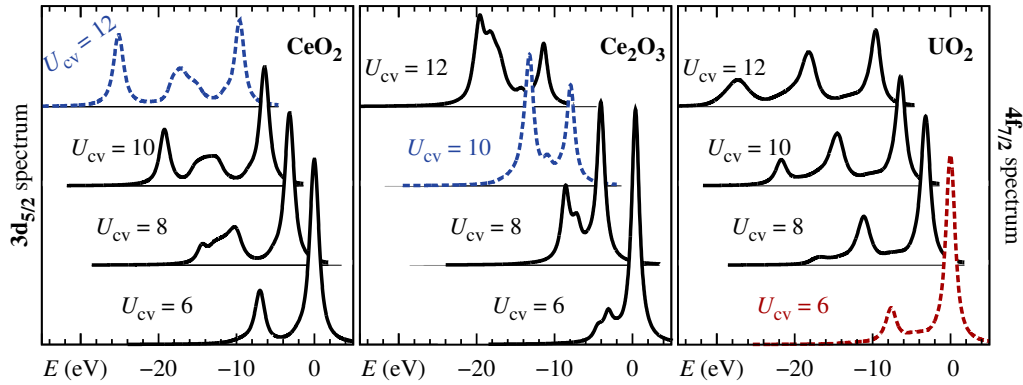|	CeO$_2$			Ce$_2$O$_3$			UO$_2$		
n	0	1	2	0	1	2	2	3	4
w_n	0.59	0.38	0.03	0.003	0.900	0.090	0.57	0.38	0.05

Figure 4: Variation of XPS due to changes of the core-valence Coulomb interaction U_{cv}. The realistic cases presented in Figure 2 and in Figure 3 are plotted with dashed lines. The broadening of the Ce$_2$O$_3$ spectrum is smaller than in Figure 3.

satellite and the sensitivity to the number of valence f electrons is lost.

Sometimes, it is possible to extract the whole valence histogram from the core spectra, that is, to determine the weights w_n of the individual charge configurations mixed in the ground state of the valence f shell [27]. Such histograms are listed in Table 2 for the oxides analyzed in Figure 4. Apparently, there is no direct correspondence between the weights w_n and the intensities of the XPS peaks in the lanthanide oxides, and even less so in the actinide oxides. A detailed calculation, taking into account the competition of the Coulomb interaction and the hybridization, has to be performed to find the connection between the XPS shape and the valence histogram. The peaks in the spectrum and their weights would directly reflect the valence histogram only if the hybridization in the final state of the photoemission process were negligible in comparison to the core-valence interaction U_{cv}. Such negligible hybridization was implicitly assumed in the recent determination of the valence histogram in plutonium metal and in several plutonium compounds [28]. Although the hybridization is indeed smaller in elemental plutonium than in, say, PuO$_2$, the condition $\Delta \ll U_{cv}$ is not fulfilled.

4. Conclusions

We have demonstrated that an implementation of the LDA+DMFT method where the self-energy is obtained by the exact diagonalization of a finite impurity model provides an accurate description of the electronic structure of selected lanthanide oxides in the paramagnetic phase.

Combining these results with our earlier study of actinide dioxides, we conclude that the core-valence Coulomb interaction in the actinide oxides is not strong enough to allow for an unambiguous determination of the filling of the 5f shell from the core-level spectra.

References

[1] J. Kolorenč, A. B. Shick, and A. I. Lichtenstein, *Electronic structure and core-level spectra of light actinide dioxides in the dynamical mean-field theory*, Phys. Rev. B **92**, 085125 (2015), arXiv:1504.07979 [cond-mat.str-el].

[2] A. Kotani and H. Ogasawara, *Theory of core-level spectroscopy of rare-earth oxides*, J. Electron. Spectrosc. and Relat. Phenom. **60**, 257–299 (1992).

[3] A. Kotani, K. Kvashnina, S. Butorin, and P. Glatzel, *Spectator and participator processes in the resonant photon-in and photon-out spectra at the Ce L$_3$ edge of CeO$_2$*, Eur. Phys. J. B **85**, 257 (2012).

[4] J. G. Tobin, S.-W. Yu, C. H. Booth, T. Tyliszczak, D. K. Shuh, G. van der Laan, D. Sokaras, D. Nordlund, T.-C. Weng, and

P. S. Bagus, *Oxidation and crystal field effects in uranium*, Phys. Rev. B **92**, 035111 (2015).

[5] P. Blaha, K. Schwarz, G. K. H. Madsen, D. Kvasnicka, and J. Luitz, *WIEN2k, An Augmented Plane Wave + Local Orbitals Program for Calculating Crystal Properties* (Techn. Universität Wien, Austria, 2001).

[6] J. Kuneš, R. Arita, P. Wissgott, A. Toschi, H. Ikeda, and K. Held, *Wien2wannier: From linearized augmented plane waves to maximally localized Wannier functions*, Comput. Phys. Commun. **181**, 1888–1895 (2010), arXiv:1004.3934 [cond-mat.mtrl-sci].

[7] A. A. Mostofi, J. R. Yates, Y.-S. Lee, I. Souza, D. Vanderbilt, and N. Marzari, *wannier90: A tool for obtaining maximally-localised Wannier functions*, Comput. Phys. Commun. **178**, 685–699 (2008), arXiv:0708.0650 [cond-mat.mtrl-sci].

[8] H. Pinto, M. Mintz, M. Melamud, and H. Shaked, *Neutron diffraction study of Ce_2O_3*, Phys. Lett. A **88**, 81–83 (1982).

[9] P. Villars, *Pearson's Handbook Desk Edition: Crystallographic Data for Intermetallic Phases* (ASM International, Materials Park, Ohio, 1997).

[10] M. Faucher, J. Pannetier, Y. Charreire, and P. Caro, *Refinement of the Nd_2O_3 and Nd_2O_2S structures at 4 K*, Acta Cryst. B **38**, 344–346 (1982).

[11] L. Gerward, J. Staun Olsen, L. Petit, G. Vaitheeswaran, V. Kanchana, and A. Svane, *Bulk modulus of CeO_2 and PrO_2—An experimental and theoretical study*, J. Alloys Compd. **400**, 56–61 (2005).

[12] A. I. Shelykh, A. V. Prokofiev, and B. T. Melekh, , Fiz. Tverd. Tela **38**, 427–432 (1996).

[13] A. V. Prokofiev, A. I. Shelykh, and B. T. Melekh, *Periodicity in the band gap variation of Ln_2O_3 (X = O, S, Se) in the lanthanide series*, J. Alloys Compd. **242**, 41–44 (1996).

[14] X. Lu, X. Li, F. Chen, C. Ni, and Z. Chen, *Hydrothermal synthesis of prism-like mesocrystal CeO_2*, J. Alloys Compd. **476**, 958–962 (2009).

[15] L. V. Pourovskii, B. Amadon, S. Biermann, and A. Georges, *Self-consistency over the charge density in dynamical mean-field theory: A linear muffin-tin implementation and some physical implications*, Phys. Rev. B **76**, 235101 (2007), arXiv:0705.2161 [cond-mat.str-el].

[16] A. Georges, G. Kotliar, W. Krauth, and M. J. Rozenberg, *Dynamical mean-field theory of strongly correlated fermion systems and the limit of infinite dimensions*, Rev. Mod. Phys. **68**, 13–125 (1996), arXiv:cond-mat/9510091.

[17] D. Jacob, K. Haule, and G. Kotliar, *Combining the hybrid functional method with dynamical mean-field theory*, EPL **84**, 57009 (2008), arXiv:0805.1383 [cond-mat.mtrl-sci].

[18] H. Jiang, P. Rinke, and M. Scheffler, *Electronic properties of lanthanide oxides from the GW perspective*, Phys. Rev. B **86**, 125115 (2012).

[19] H.-D. Kim, H.-J. Noh, K. H. Kim, and S.-J. Oh, *Core-level x-ray photoemission satellites in ruthenates: A new mechanism revealing the Mott transition*, Phys. Rev. Lett. **93**, 126404 (2004), arXiv:cond-mat/0403066 [cond-mat.str-el].

[20] F. de Groot and A. Kotani, *Core Level Spectroscopy of Solids* (CRC Press, Boca Raton, FL, 2008).

[21] A. Kotani and T. Yamazaki, *Systematic analysis of core photoemission spectra for actinide di-oxides and rare-earth sesqui-oxides*, Prog. Theor. Phys. Supplement **108**, 117–131 (1992).

[22] E. Wuilloud, B. Delley, W. D. Schneider, and Y. Baer, *Spectroscopic evidence for localized and extended f-symmetry states in CeO_2*, Phys. Rev. Lett. **53**, 202–205 (1984).

[23] Y. Baer and J. Schoenes, *Electronic structure and Coulomb correlation energy in UO_2 single crystal*, Solid State Commun. **33**, 885–888 (1980).

[24] B. W. Veal, D. J. Lam, H. Diamond, and H. R. Hoekstra, *X-ray photoelectron-spectroscopy study of oxides of the transuranium elements Np, Pu, Am, Cm, Bk, and Cf*, Phys. Rev. B **15**, 2929–2942 (1977).

[25] L. E. Roy, T. Durakiewicz, R. L. Martin, J. E. Peralta, G. E. Scuseria, C. G. Olson, J. J. Joyce, and E. Guziewicz, *Dispersion in the Mott insulator UO_2: A comparison of photoemission spectroscopy and screened hybrid density functional theory*, J. Comput. Chem. **29**, 2288–2294 (2008).

[26] J. C. Fuggle, M. Campagna, Z. Zolnierek, R. Lässer, and A. Platau, *Observation of a relationship between core-level line shapes in photoelectron spectroscopy and the localization of screening orbitals*, Phys. Rev. Lett. **45**, 1597–1600 (1980).

[27] J.-P. Rueff, J.-P. Itié, M. Taguchi, C. F. Hague, J.-M. Mariot, R. Delaunay, J.-P. Kappler, and N. Jaouen, *Probing the $\gamma-\alpha$ transition in bulk Ce under pressure: A direct investigation by resonant inelastic x-ray scattering*, Phys. Rev. Lett. **96**, 237403 (2006), arXiv:cond-mat/0602169 [cond-mat.str-el].

[28] C. Booth, S. Medling, Y. Jiang, E. Bauer, P. Tobash, J. Mitchell, D. Veirs, M. Wall, P. Allen, J. Kas, D. Sokaras, D. Nordlund, and T.-C. Weng, *Delocalization and occupancy effects of 5f orbitals in plutonium intermetallics using L_3-edge resonant X-ray emission spectroscopy*, J. Electron. Spectrosc. Relat. Phenom. **194**, 57–65 (2014).